



Estimation of nonlinear dependence of fiber Bragg grating readings on temperature and strain using experimental data

I. Shardakov, A. Shestakov, I. Glot, V. Epin, G. Gusev, R. Tsvetkov

Institute of Continuous Media Mechanics, Ural Branch, Russian Academy of Science, 1, Korolev street, Perm, Russia

shardakov@icmm.ru, <https://orcid.org/0000-0001-8673-642X>

shap@icmm.ru, <https://orcid.org/0000-0003-3387-7442>

glot@icmm.ru, <https://orcid.org/0000-0002-2842-7511>

epin.v@icmm.ru, <https://orcid.org/0000-0001-5625-2678>

gusev.g@icmm.ru, <https://orcid.org/0000-0002-9072-0030>

flower@icmm.ru, <https://orcid.org/0000-0001-9617-407X>

ABSTRACT. The readings of the Bragg grating are determined based on the optical radiation reflected from it. A quantitative characteristic of this radiation is the wavelength at which the maximum power of the optical signal is achieved. This characteristic is called the central wavelength of the grating. The central wavelength shift depends on temperature and strain. As a rule, a linear approximation of this dependence is used. However, from the available literature it is known that, the grating wavelength shift demonstrates a strong nonlinear dependence on temperature at $5 < T < 200\text{K}$ and a weak quadratic dependence close to room temperature. Thus far, the authors have not found studies that consider all terms in the quadratic expansion of the central wavelength of the Bragg grating as a function of temperature and strain at near-room temperatures. Our work is intended to fill this gap. The article describes an experiment in which an optical fiber with Bragg grating was subjected to loading using three different weights. A step-wise temperature change from 5 to 100 °C was realized for each weight. Based on these data, all terms of the quadratic expansion of the desired function are determined. The contribution of each term is estimated.

KEYWORDS. Fiber Bragg grating; Sensor calibration; Temperature compensation; Quadratic approximation.



Citation: Shardakov, I., Shestakov, A., Glot, I., Epin, V., Gusev, G., Tsvetkov, R., Estimation of the nonlinear dependence of the indications of a fiber Bragg grating on temperature and strain from experimental data, *Frattura ed Integrità Strutturale*, 62 (2022) 561-572.

Received: 02.07.2022

Accepted: 09.09.2022

Online first: 13.09.2022

Published: 01.10.2022

Copyright: © 2022 This is an open access article under the terms of the CC-BY 4.0, which permits unrestricted use, distribution, and reproduction in any medium, provided the original author and source are credited.

INTRODUCTION

The fiber Bragg gratings are used as optical temperature and strain sensors. Optical sensors have a number of advantages over traditional measuring facility: optical sensors are not sensitive to electromagnetic interference, can be easily create long measuring lines, allow switching of many sensors on one measuring line, have very small size and weight, have low heat capacity, the optical line has a low thermal conductivity, line and sensor demonstrate high

explosion resistance. Due to these advantages, optical sensors have found wide application in the monitoring of buildings, bridges, pipelines, mines and tunnels due to their great length. Fiber optic sensors are widely used for monitoring composite materials, as they can be embedded in the material without weakening its strength characteristics due to small sizes of sensors and measuring line. A variety of sensing devices such as the displacement, strain, pressure, acceleration and temperature sensors are created based on the fiber Bragg gratings. The fields of application of fiber Bragg sensors are described in [1, 2].

The readings of the Bragg grating sensor are calculated based on the shift of the central wavelength of the grating. This index depends on temperature and strain. Generally, it is not known, which of these factors causes the wavelength shift so there is a measurement uncertainty. As a rule, temperature measurements are conducted at a free state of the fiber within the grating area, when it is not subjected to external loads. In this case, the strain is known and is expressed in terms of temperature. For strain measurements different methods are used [3]. The simplest and most reliable method is to use two gratings: one grating is attached to the test object and the second grating is freely located near the first one [4]. In this case, temperature sensing is provided by the second grating. Knowing the temperature and wavelength shift of the first grating it is possible to evaluate its strain. One further implementation of this approach is based on the method, in which a Bragg grating designed to determine temperature is attached to a metal plate with a known coefficient of thermal expansion. Another method that implements the use of two gratings is that the gratings are fixed in the stretched and compressed zones of the sensor, in this case the difference in wave shifts does not depend on temperature [5,6]. There are also many techniques that do not require maintaining a special mechanical state of one of the gratings [7-13]. These methods use not only a shift of the grating spectrum, but also a change in the shape of this spectrum or changes in the amplitudes of parts of the spectrum.

The individual calibration of grating can be reasonably done in the following cases: temperature compensation is performed based on the temperature measured by any means; sensor design is supposed to maintain a free state of the fiber in the Bragg grating area; sensor design does not allow individual calibration of the sensor assembly. This is especially true for high-precision strain gauges, the design of which involves fiber attachment by soldering or welding the metal-coated fiber [3]. In this case, long-term stability of measurements is achieved.

As a rule, the calibration of Bragg grating sensors is carried out in the framework of a linear approximation [3, 5-15]. Although there has been experimental evidence that the temperature dependence of a shift of the central wavelength of the grating has a strongly nonlinear character at $5 < T < 200$ K [1,16,17]. There are also studies, which have established a reliably measured quadratic dependence of the grating wavelength shift on temperature at $-30 < T < 80$ °C [18,19]. In [18], an explanation of the temperature dependent non-linear behavior of the fiber Bragg grating is given based on the Ghosh model, which relates the non-linear behavior of the refractive index of quartz glass to temperature. Note that in addition to nonlinearity associated with temperature, there is nonlinearity due to deformation. This is shown in [18]. The authors of this work conducted an experiment, in which the fiber was subjected to loading at constant temperature and plotted graphs of the error of a linear approximation of the dependence of the wavelength shift on strain. As is evident from this graph, there is a weak negative quadratic dependence. However, they did not quantify this relationship. Thus, for near-room temperatures the present-day literature provides comprehensive information on the linear terms of the expansion of the grating wavelength shift $\Delta\lambda$ as the function of strain $C_1 \cdot \varepsilon$ and temperature $C_2 \cdot \Delta T$, there are estimates for the quadratic expansion term $C_4 \cdot \Delta T^2$. However, we have not found any information on the consideration of quadratic $C_3 \cdot \varepsilon^2$ and cross $C_1 \cdot \varepsilon \cdot \Delta T$ terms of the expansion. Our paper is intended to fill this gap.

The paper is structured as follows. Section 1 describes the principle of operation of the fiber Bragg grating and provides substantiation of parameters used to make calibration. Section 2 describes the experimental setup. The experimental results and the data processing algorithm are discussed in Section 3. The parameters of the full quadratic approximation are determined in Section 4. The last Section summarizes the results obtained.

THE WORKING PRINCIPLE OF THE FIBER BRAGG GRATING

The Bragg grating is a region of an optical fiber, in which the refractive index periodically changes. The period of this structure is called the period of the Bragg grating. A structural diagram of the grating is shown in Fig. 1. The fiber area with applied grating reflects a narrow part of the optical radiation spectrum, which is determined by the grating period, the stress-strain state of the fiber in the grating area, and temperature. The measurement process involves the generation of a broadband optical signal and the registration of the reflected spectrum.

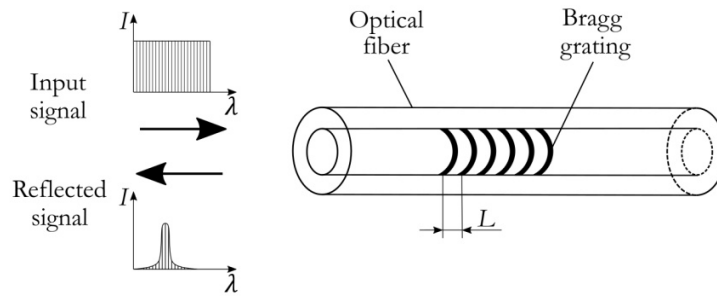


Figure 1: Structural diagram of the Bragg grating in an optical fiber.

The sensor indications are determined by the shift of the spectrum of the reflected optical signal. Two spectra of the optical signal are shown in Fig. 2. Spectrum 1 corresponds to the grating in the initial state, spectrum 2 - to the deformed state. The spectra are characterized by their central wavelengths λ_1 and λ_2 . The shift of the spectrum is quantified by the change in the central wavelength $\Delta\lambda = \lambda_2 - \lambda_1$.

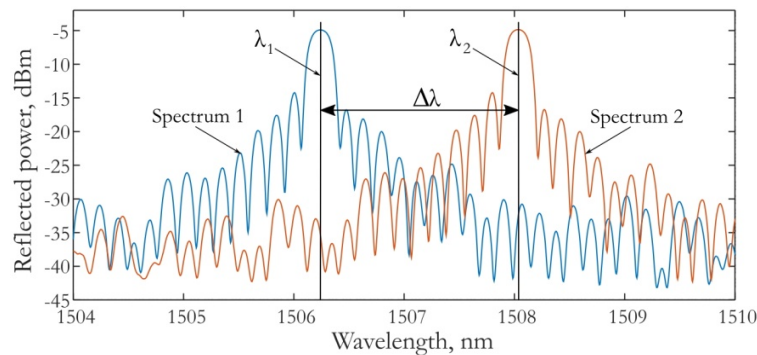


Figure 2: Spectra of optical signals (spectrum 1 - grating in the initial state, spectrum 2 - grating in the deformed state)

The central wavelength of the grating is determined by the expression

$$\lambda = 2 \cdot n(T, \boldsymbol{\varepsilon}) \cdot L(\boldsymbol{\varepsilon}_l) \tag{1}$$

where: $n(T, \boldsymbol{\varepsilon})$ is the refractive index of quartz in the grating area; T is temperature; $\boldsymbol{\varepsilon}$ is the strain tensor of the fiber in the grating area; L is the grating period; $\boldsymbol{\varepsilon}_l$ is the total strain along the fiber. Let us define the reference state of the grating, which is characterized by zero strains, the reference state temperature T_0 , and the grating period in the reference state L_0 . The wavelength in the reference state is defined by

$$\lambda_0 = 2 \cdot n(T_0, \mathbf{0}) \cdot L_0 = 2 \cdot n_0 \cdot L_0 \tag{2}$$

where: n_0 is the refractive index in the reference state. The current value of the refractive index represented in increments relative to the reference state is written as

$$n(T, \boldsymbol{\varepsilon}) = n(T_0, \mathbf{0}) + \Delta n(T - T_0, \boldsymbol{\varepsilon}) = n_0 + \Delta n \tag{3}$$

where: Δn – is the increment of the refractive index. The grating period in the actual (deformed) state is determined by the expression

$$L(\boldsymbol{\varepsilon}_l) = L_0 \cdot (1 + \boldsymbol{\varepsilon}_l) \tag{4}$$

The wave length in the actual state (1), according to expressions (3) and (4) takes the following form



$$\lambda = 2 \cdot (n_0 + \Delta n) \cdot L_0 \cdot (1 + \varepsilon_l) \tag{5}$$

After opening the brackets we get

$$\lambda = 2 \cdot n_0 \cdot L_0 + 2 \cdot n_0 \cdot L_0 \cdot \varepsilon_l + 2 \cdot \Delta n \cdot L_0 \cdot (1 + \varepsilon_l) \tag{6}$$

The multiplication of the numerator and denominator of the summand at Δn by n_0 yields

$$\lambda = \frac{2 \cdot n_0 \cdot L_0}{n_0} + \frac{2 \cdot n_0 \cdot L_0 \cdot \varepsilon_l}{n_0} + \frac{2 \cdot n_0 \cdot L_0 \cdot (1 + \varepsilon_l) \cdot \Delta n}{n_0} \tag{7}$$

The underlined expressions according to (2) are the central wavelengths of the grating in the reference state

$$\lambda = \lambda_0 + \lambda_0 \cdot \varepsilon_l + \lambda_0 \cdot (1 + \varepsilon_l) \cdot \frac{\Delta n}{n_0} \tag{8}$$

Using simple arithmetic operations, expression (8) is transformed to

$$\frac{\lambda - \lambda_0}{\lambda_0} = \varepsilon_l + (1 + \varepsilon_l) \cdot \frac{\Delta n}{n_0} \tag{9}$$

The resulting expression determines the relative change in the wavelength. From this expression we can draw an important conclusion that the relative change in the wavelength is independent of the grating period in the reference configuration L_0 . The refractive index increment depends on the strain and temperature $\Delta n = \Delta n(T - T_0, \varepsilon)$, so that

$$\frac{\lambda - \lambda_0}{\lambda_0} = \varepsilon_l + (1 + \varepsilon_l) \cdot \frac{\Delta n(T - T_0, \varepsilon)}{n_0} = f(T - T_0, \varepsilon, n_0) \tag{10}$$

The expression $f(T - T_0, \varepsilon, n_0)$ depends on the temperature, strain and refractive index of the optical fiber in the reference configuration $n_0 = n(T_0, \theta)$. Under the same conditions of determining the reference configuration $\varepsilon = 0$ and $T = T_0$, for the same type of optical fiber and the same technology of applying the grating on the fiber, the quantity n_0 will be a constant. It follows from the above that

$$\frac{\lambda - \lambda_0}{\lambda_0} = f(T - T_0, \varepsilon) \tag{11}$$

Under the described conditions, dependence (11) will be valid for gratings with different periods. In the case when the side surface of the fiber in the region of the Bragg grating is free (not stressed), the radial and circumferential deformations of the fiber depend only on temperature and deformation along the fiber. Under these conditions, the remaining components of the strain tensor ε are equal to zero. Therefore, (11) takes the form

$$\frac{\lambda - \lambda_0}{\lambda_0} = f(T - T_0, \varepsilon_l) \tag{12}$$

In the quadratic approximation function $f(T - T_0, \varepsilon_l)$ is written as

$$f(T - T_0, \varepsilon_l) = C_1 \cdot \varepsilon_l + C_2 \cdot (T - T_0) + C_3 \cdot \varepsilon_l^2 + C_4 \cdot (T - T_0)^2 + C_5 \cdot \varepsilon_l \cdot (T - T_0) \tag{13}$$

In what follows, we will describe the experiments that allow us to determine the parameters of this expansion.

DESCRIPTION OF EXPERIMENTAL SETUP

The photograph of the experimental setup is shown in Fig.3 It consists of a glass cylindrical vessel 1, on which a nichrome wire 6 is evenly wound to provide its heating and maintain the prescribed temperature. Air inside the vessel is stirred to ensure the uniform temperature distribution. In the process of stirring, the air is drawn in by the turbine 3 in the lower part of the vessel, and then it moves through the aluminum tube 7 into the chamber in the upper part of the vessel 8. After that, the air returns to the working area of the vessel through the perforated plate. From above the vessel is plugged with seal 9, which does not allow the air from the environment to get into the vessel. From below it is protected by insulating pad 2 to reduce a heat flux through the bottom. Inside the vessel there is an optical fiber with a Bragg grating 11. Fiber is loaded with a set of weights 4. Attachment to the fiber is by means of grip 5. Through the distributing plate 13 the fiber is clamped between rubber pads 14. Compressive force is produced by elastic clamp 12. To reduce the compressive force in the clamp 12 to a level that ensures no damage to the fiber, a ring element is provided in the grip 5. This reduction in clamping force is achieved due to the frictional forces generated by winding the fiber around the annular part. Changing the amount of winding makes it easy to adjust the axial force in the fiber with a constant compressive force in the clamp 12. The temperature sensor 10 is brought to the fiber in the region of the Bragg grating 11 at a distance of 1-2 mm. To minimize the influence of the environment, during the experiment the vessel is placed inside a cube made of 50 mm thick foam plastic.

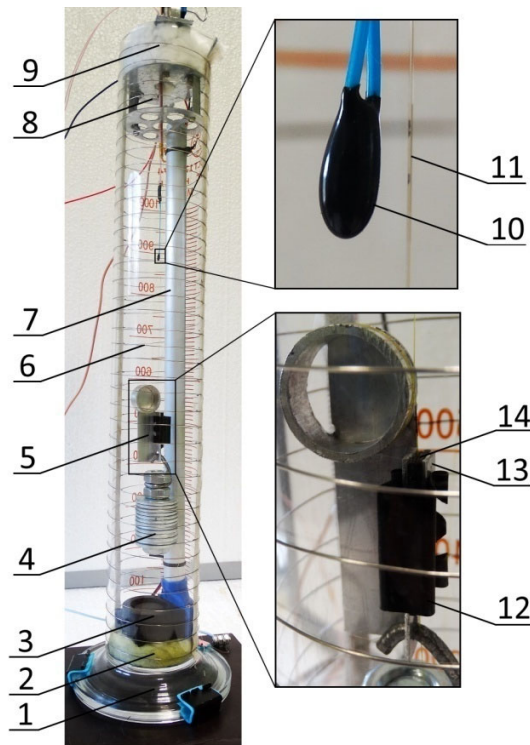


Figure 3: Experimental setup.

Power supply to the heating wire is regulated with a microcontroller and an external circuit on a field-effect transistor. The microcontroller is controlled by a computer, which measures temperature. A special computer program was developed to implement the PID regulation algorithm, which maintains the prescribed temperature inside the vessel and operates the step-wise temperature loading.

The generation of a broadband optical signal and recording of the spectra reflected from the Bragg grating were accomplished using the ASTRO A322 interrogator manufactured by FiberSensing. The Bragg grating is fabricated in a single-mode fiber of the SM1500(9-125)P series. The initial grating wavelength is 1525 nm. Temperature registration is performed using the B57861-S 103-F40 thermistor manufactured by EPCOS. The thermistor resistance is measured with a 24-bit Leonardo 2 ADC and a GSPF-052 generator manufactured by Rudnev-Shilyaev producer. Synchronization of

temperature measurements and spectra of the Bragg grating is provided automatically using a specially developed program in the Delphi language. The temperature sensor is calibrated with TL-4 mercury thermometers, which have two temperature scales of 0-50 and 50-100 °C. The division value of thermometers and, as a result, the calibration accuracy is 0.1 degrees.

EXPERIMENT PROCEDURE AND DATA PROCESSING

The experiment includes two operations: hanging of weights an optical fiber and setting temperature from 5 to 100 °C with an increment of 5 °C. The temperature in the thermal chamber is set in steps with an exposure time of 15 minutes per step. In the area of the Bragg grating, the insulation was removed from the fiber to eliminate the influence of the polymer shell. The weight sets the elastic deformation ϵ_0 in the grating region, which does not change with temperature. We performed a set of experiments with three different weights ($m_1=29.040g$, $m_2=109.975g$, $m_3=216.431g$), which allowed us to determine all parameters of the quadratic approximation. The strains ϵ_0 , corresponding to these weights were $321\mu\epsilon$, $1216\mu\epsilon$, $2395\mu\epsilon$, respectively. Evolution of the temperature and the corresponding change in the central wavelength of the grating at several stages of temperature loading are shown in Fig. 4.

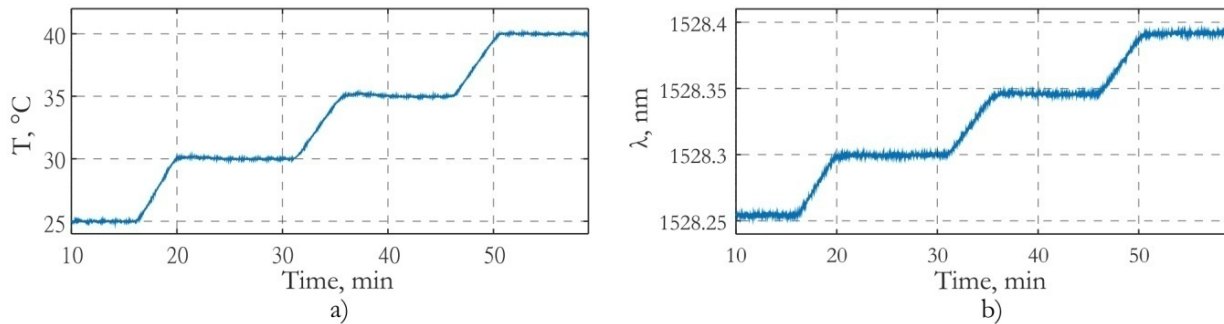


Figure 4: Evolution of temperature (a) and Bragg grating wavelength (b) as a function of time.

At each step, the readings were averaged over two minutes. The averaged values were used to plot the grating wavelength versus temperature (Fig. 5) at different initial strains ϵ_0 .

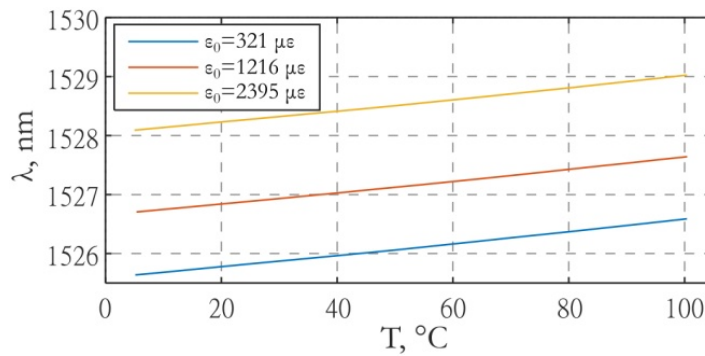


Figure 5: Dependence of the grating wavelength on temperature at different initial strains ϵ_0 .

Quite often, the central wavelength of the Bragg grating is determined from the maximum of the spectrum. However, this approach does not provide stable results. This is illustrated by the spectrum graphs (Fig. 6a) obtained from 4 consecutive measurements at constant temperature and strain. It can be seen from these plots that the wavelength at which the maximum value is reached may differ from one measurement to the next. To overcome this difficulty, an algorithm is proposed that determines the value of the central wavelength as the wavelength corresponding to the centre of mass of a figure bounded by points A, B, C (fig.6b). Point B corresponds to the maximum of the spectrum, and points A and C are closest to B, where value 20 dB below the maximum is achieved.

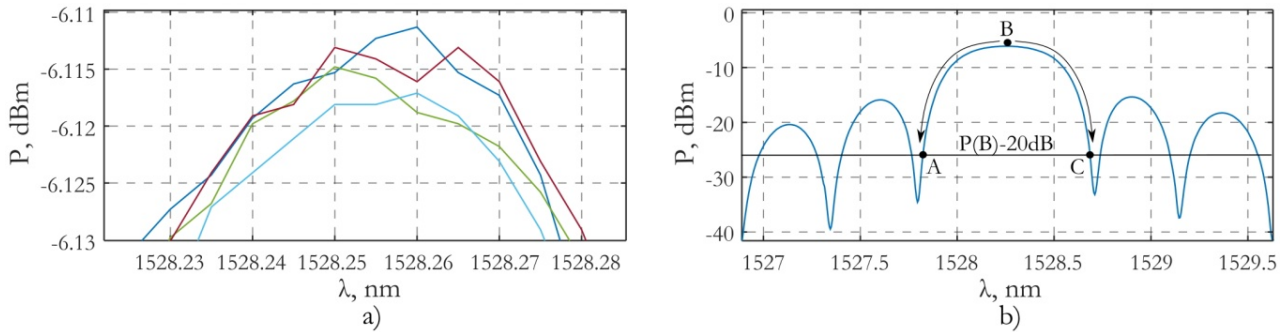


Figure 6: The shapes of the spectral maxima for four consecutive measurements at constant temperature and deformation (a), the search algorithm for the central wavelength of the Bragg grating (b).

The developed algorithm can significantly reduce the processed data scattering and increase the sensitivity of the measuring system. This is clearly seen in Fig. 7, which shows the evolution of the central wavelengths determined by means of direct registration of the spectrum maximum (Fig. 7a) and calculation of the centre of mass (Fig. 7b). According to these graphs, the developed algorithm reduces the scatter of the processed data by a factor of 10. It should be noted that the developed algorithm and time averaging over an interval of 1 minute (60 measurements) allowed us to obtain the wavelength sensitivity of $\approx 0.1 \mu m$.

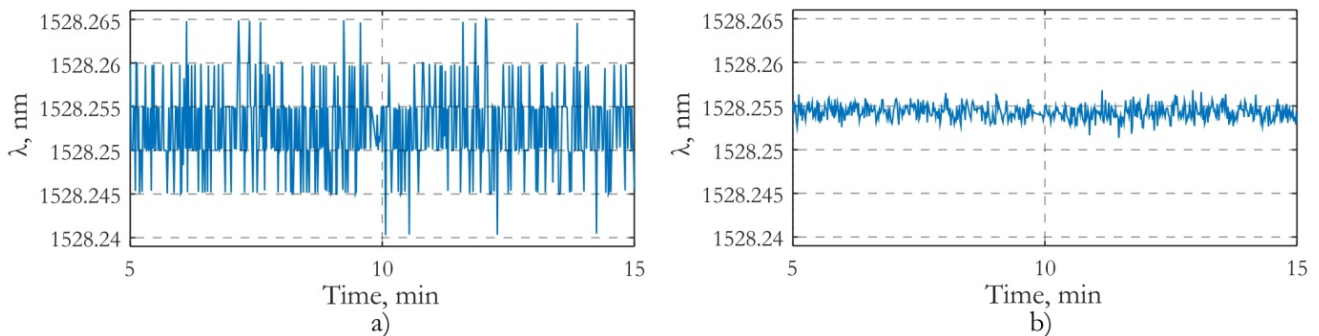


Figure 7: Wavelengths calculated with the use of the algorithms based on spectrum maximum (a) and centre of mass (b).

DETERMINATION OF PARAMETERS OF QUADRATIC APPROXIMATION

The approximation of the function describing the relative wavelength change is expressed as follows

$$f(\Delta T, \varepsilon) = C_1 \cdot \varepsilon + C_2 \cdot \Delta T + C_3 \cdot \varepsilon^2 + C_4 \cdot \Delta T^2 + C_5 \cdot \varepsilon \cdot \Delta T \quad (14)$$

where $\Delta T = T - T_0$. Here, unlike Eqn. (13), the lower index of ε is omitted. The longitudinal strain ε of a fiber stretched by applying a weight of mass m under conditions of variable temperature is given as

$$\varepsilon = \varepsilon_0 + \alpha \cdot \Delta T \quad (15)$$

where: ε_0 is the strain of the fiber due to the applied weight; α – is the coefficient of linear expansion of quartz equal to $0.54 \cdot 10^{-6} \text{ 1/}^\circ\text{C}$. The deformation ε_0 is determined using the expressions

$$\varepsilon_0 = \frac{\sigma_l}{E}, \sigma_l = \frac{m \cdot g}{S}, S = \frac{\pi \cdot D^2}{4} \quad (16)$$



where: σ_f is the stress along the fiber; E is Young's module of quartz equal to $72.3 \cdot 10^9$ Pa; m is the mass of the weight; g is the acceleration of gravity equal to 9.81 m/s²; D is the diameter of the fiber equaling to 125 μm ; S is the fiber cross-sectional area.

Based on the results of experiments, three tabular dependencies were obtained

$$(\Delta T_i^j, \lambda_i^j) \tag{17}$$

where: j determines the belonging to the corresponding weight and varies from 1 to 3; i indicates the belonging to a given temperature and varies from 1 to 20. Using expression (15), we can calculate the strains corresponding to weights j and temperatures i .

$$\varepsilon_i^j = \varepsilon_0^j + \alpha \cdot \Delta T_i^j \tag{18}$$

Using the least squares method, we perform series expansion of the dependence of the central wavelength on deformation and temperature.

$$\lambda(\Delta T, \varepsilon) = q_0 + q_1 \cdot \varepsilon + q_2 \cdot \Delta T + q_3 \cdot \varepsilon^2 + q_4 \cdot \Delta T^2 + q_5 \cdot \varepsilon \cdot \Delta T \tag{19}$$

To this end we introduce the following row vectors

$$\begin{aligned} \mathbf{1} &= [1 \quad \dots \quad 1] \\ \boldsymbol{\varepsilon} &= [\varepsilon_1^1 \quad \dots \quad \varepsilon_N^1 \quad \varepsilon_1^2 \quad \dots \quad \varepsilon_N^2 \quad \varepsilon_1^3 \quad \dots \quad \varepsilon_N^3] \\ \Delta \mathbf{T} &= [\Delta T_1^1 \quad \dots \quad \Delta T_N^1 \quad \Delta T_1^2 \quad \dots \quad \Delta T_N^2 \quad \Delta T_1^3 \quad \dots \quad \Delta T_N^3] \\ \boldsymbol{\lambda} &= [\lambda_1^1 \quad \dots \quad \lambda_N^1 \quad \lambda_1^2 \quad \dots \quad \lambda_N^2 \quad \lambda_1^3 \quad \dots \quad \lambda_N^3] \end{aligned} \tag{20}$$

where $\mathbf{1}$ is the unit row vector of size $3 \cdot N$; N is the number of points of temperature loading, which is equal to 20. The introduced vectors are used to generate a matrix of the following form

$$\mathbf{M} = \begin{bmatrix} \mathbf{1} \\ \boldsymbol{\varepsilon} \\ \Delta \mathbf{T} \\ \boldsymbol{\varepsilon} \circ \boldsymbol{\varepsilon} \\ \Delta \mathbf{T} \circ \Delta \mathbf{T} \\ \boldsymbol{\varepsilon} \circ \Delta \mathbf{T} \end{bmatrix} \tag{21}$$

where: \circ is the component product. According to least squares method, the system of linear algebraic equations with respect to the approximation parameters of expression (19) is represented as

$$(\mathbf{M} \cdot \mathbf{M}^T) \cdot \mathbf{q} = (\mathbf{M} \cdot \boldsymbol{\lambda}^T) \tag{22}$$

where: \cdot is the scalar product; T is the transposition operator; \mathbf{q} is the column vector of the approximation parameters. The approximation parameter q_j is equal to the central wavelength of the grating in the reference configuration ($\Delta T=0, \varepsilon=0$)

$$\lambda_0 = q_0 \tag{23}$$

To calculate the relative change in the wavelength using expression (19), we must subtract λ_0 from it and divide it by λ_0 .



$$\frac{\lambda(\Delta T, \varepsilon) - \lambda_0}{\lambda_0} = \frac{q_0 - q_0}{q_0} + \frac{q_1}{q_0} \cdot \varepsilon + \frac{q_2}{q_0} \cdot \Delta T + \frac{q_3}{q_0} \cdot \varepsilon^2 + \frac{q_4}{q_0} \cdot \Delta T^2 + \frac{q_5}{q_0} \cdot \varepsilon \cdot \Delta T \quad (24)$$

Comparing expressions (14) and (24) we obtain the coefficients of required expansion (14)

$$C_1 = \frac{q_1}{q_0}, C_2 = \frac{q_2}{q_0}, C_3 = \frac{q_3}{q_0}, C_4 = \frac{q_4}{q_0}, C_5 = \frac{q_5}{q_0} \quad (25)$$

They have the following values:

$$C_1 = 0.782, C_2 = 5.66 \cdot 10^{-6}, C_3 = -2.49, C_4 = 7.03 \cdot 10^{-9}, C_5 = -6.31 \cdot 10^{-5} \quad (26)$$

Let us consider the expansion error (14) with respect to the initial experimental data (17), (18). It is determined by expression (27).

$$\delta_i^j = \frac{\lambda_i^j - \lambda_0}{\lambda_0} - f(\Delta T_i^j, \varepsilon_i^j) \quad (27)$$

Graphs of the approximation error (27) are shown in Fig. 8. These graphs correspond to three weights $j=1,2,3$, which set the initial deformation $\varepsilon_0 = 321 \mu\varepsilon, 1216 \mu\varepsilon, 2395 \mu\varepsilon$.

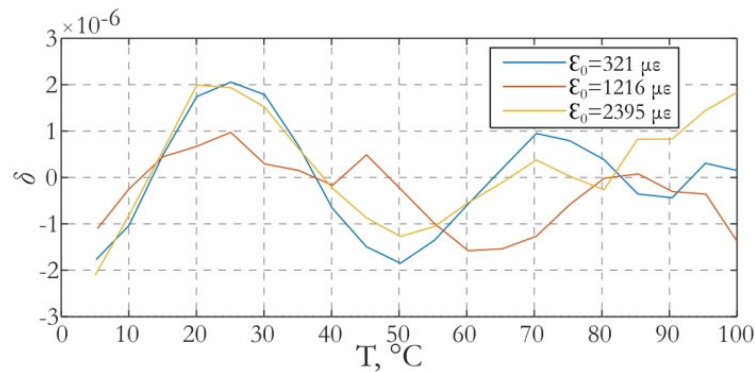


Figure 8: Approximation error for three levels of initial strain and temperature variations from 5 to 100 °C

The graph shows that for strains changing from 0 to 2400 $\mu\varepsilon$ and temperature changing from 5 to 100 °C the maximum error of approximation of the relative wavelength is $\delta_{max} = \pm 2 \cdot 10^{-6}$. This value corresponds to the error of strain of $\approx \pm 2.5 \mu\varepsilon$. Four fragments in Fig. 9 show how the approximation error changes depending on temperature and deformation when various terms are excluded from the expression (14). These graphs clearly demonstrate the contribution of each non-linear term. Fig. 9a shows the error, which occurs when the term $C_3 \cdot \varepsilon^2$ ($C_3=0$) is excluded from the expansion. In this case, the maximum error value was $\delta_{max} = -18 \cdot 10^{-6}$. Figs. 9b and 9c show the graphs of approximation error due to removal of terms $C_4 \cdot \Delta T^2$ and $C_5 \cdot \Delta T \cdot \varepsilon$, and Fig. 9d corresponds to the situation when all non-linear terms $C_3 \cdot \varepsilon^2, C_4 \cdot \Delta T^2, C_5 \cdot \Delta T \cdot \varepsilon$ are excluded. Based on these graphs, the following conclusions can be drawn. The largest approximation error occurs due to removal of the non-linear term $C_4 \cdot \Delta T^2$ (Fig. 9b). The maximum error value in this case is equal to $\delta_{max} = 46 \cdot 10^{-6}$. Nonlinear terms enter the expansion with different signs and partially compensate each other. Compared to the approximation error (Fig. 8), the contribution of the non-linear terms shown in Fig. 9 is substantial.

The contribution of each term of expansion (14) at temperature $\Delta T = 100$ °C and strain $\varepsilon = 2500 \mu\varepsilon$ is evaluated as

$$(1955 + 566 - 15 + 70 - 15) \cdot 10^{-6} \quad (28)$$

The contributions of the summands with respect to the first term of the expansion are expressed in percentages as (29). The parentheses indicate the belonging to the corresponding term of the expansion.

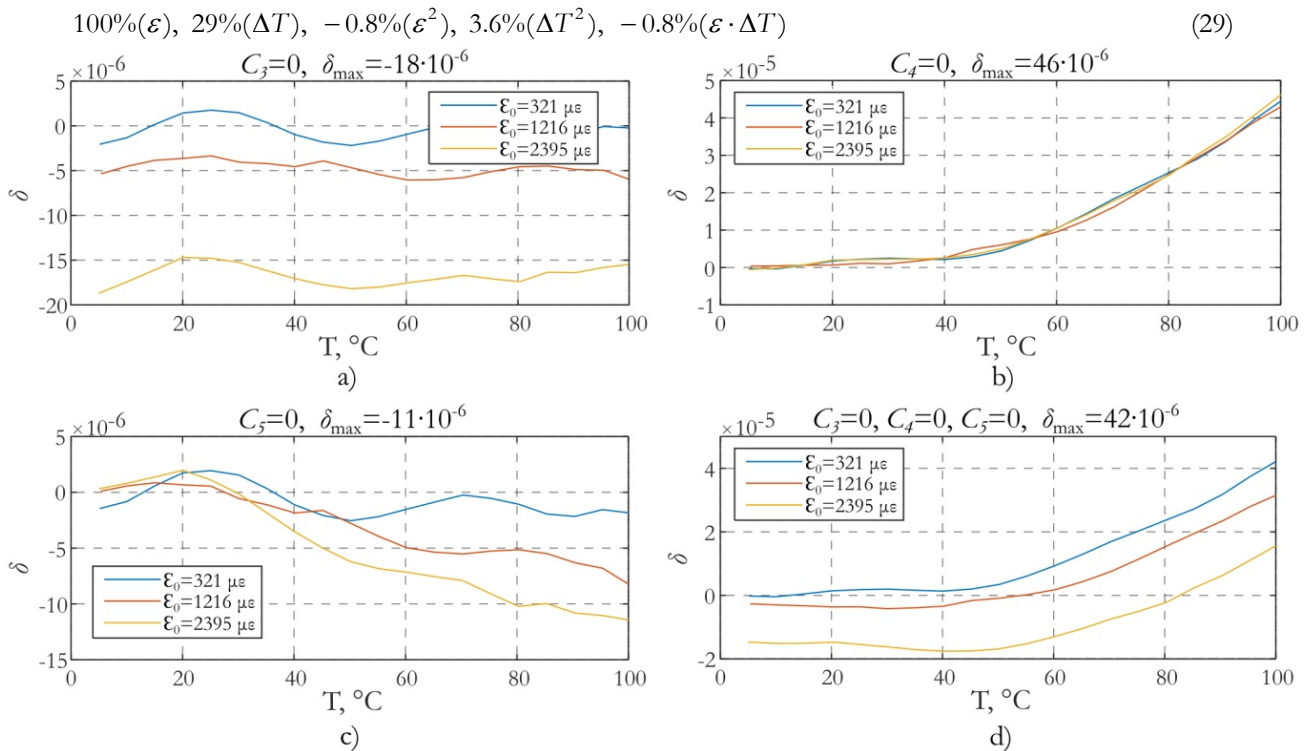


Figure 9: Graphs of approximation errors for three strain levels at different numbers of expansion terms

CONCLUSIONS

Several important conclusions follow from the analysis of the obtained ratio 14. When using sensors based on the Bragg grating to measure strain, it is necessary to take into account not only the accuracy of estimating the shift of the grating wavelength, but also the accuracy of temperature measurement. If the temperature is measured roughly, and the shift of the grating wavelength is estimated very accurately, then the accuracy of determining the deformation will be determined by the accuracy of the temperature measurement. To ensure the strain measurement accuracy of $\pm 1\mu\varepsilon$, the temperature measurement accuracy should be no worse than $\pm 0.1^\circ\text{C}$.

Comparison of the contributions of individual terms given in relation (28) makes it possible to estimate which terms of expansion (14) must be taken into account to ensure the required accuracy of the measuring system. So, if the allowable error in strain measurement is 5% or more, only linear terms can be taken into account in expansion (14). To ensure the accuracy of the measuring system of 1% or better, it is necessary to take into account the quadratic terms of the expansion.

The reliability of the obtained results can be demonstrated by comparing them with the data presented in [16]: $C_1=0.782(0.806)$, $C_2=5.66\cdot 10^{-6}(5.77\cdot 10^{-6})$, $C_4=7.03\cdot 10^{-9}(8.02\cdot 10^{-9})$. Here the values of the coefficients (26) are given, and in parentheses are the corresponding values taken from [16].

The obtained individual calibration dependence of the Bragg grating in the form of relation (14) makes it possible to evaluate how the sensor readings depend on the features of its design. In the process of creating and debugging a Bragg grating sensor, it is quite difficult to determine how the sensor readings depend on the method of fiber attachment. Having an individual calibration dependence for a particular grating, it is possible to reliably identify the contribution to the sensor readings due to fiber attachment, and take appropriate measures to reduce this value. This is especially true when creating high-precision measuring systems that provide an accuracy of 0.1% or better.

The construction of a quadratic approximation for the calibration dependence of the grating requires careful control of the parameters of the reference configuration (temperature T_0 and external mechanical stresses of the fiber, which must be



zero). To do this, it is proposed to carry out a series of successive loadings of the fiber placed in a thermostat. Loading is performed by successive suspension of weights on the fiber, which ensures the straightness of the fiber. Then the dependence of the grating wavelength on the load value is constructed. Approximation of this dependence to the zero value of the load makes it possible to obtain the value λ_0 . The calibration dependence obtained in this way is universal when using the same reference configuration, the same type of optical fiber, and the same technology for applying the grating to the fiber.

The accuracy of determining the central wavelength with the aid of modern interrogators is 1 pm. This corresponds to a strain of $\approx 0.8 \mu\epsilon$. Therefore, to ensure the full-scale realization of capabilities of modern interrogators, one should use a quadratic approximation taking into account all terms of the expansion.

ACKNOWLEDGMENTS

The paper was prepared in the framework of the program for the creation and development of the world-class scientific center «Supersonic»; for 2020-2025 with the financial support of the Ministry of Education and Science of the Russian Federation (Agreement No. 075-15-2020-925 of November 16, 2020).

REFERENCES

- [1] Wang, Y. L., Tu, Y., Tu, S. T. (2020). Development of highly-sensitive and reliable fiber Bragg grating temperature sensors with gradient metallic coatings for cryogenic temperature applications, *IEEE Sensors Journal*, 21(4), pp. 4652-4663. DOI: 10.1109/JSEN.2020.3036411.
- [2] Sarkar, S., Tarhani, M., Khosravi Eghbal, M., Shadaram, M. (2020). Discrimination between strain and temperature effects of a single fiber Bragg grating sensor using sidelobe power, *Journal of Applied Physics*, 127(11), pp. 114503. DOI: 10.1063/1.5139041.
- [3] Kuang, Y., Guo, Y., Xiong, L., Liu, W. (2018). Packaging and temperature compensation of fiber Bragg grating for strain sensing: a survey, *Photonic Sensors*, 8(4), pp. 320-331. DOI: 10.1007/s13320-018-0504-y.
- [4] Zhou, Z., Ou, J. (2005). Techniques of temperature compensation for FBG strain sensors used in long-term structural monitoring, *Fundamental Problems of Optoelectronics and Microelectronics II*, 5851, pp. 167-172. DOI: 10.1117/12.634047.
- [5] Li, R., Tan, Y., Chen, Y., Hong, L., Zhou, Z. (2019). Investigation of sensitivity enhancing and temperature compensation for fiber Bragg grating (FBG)-based strain sensor, *Optical Fiber Technology*, 48, pp. 199-206. DOI: 10.1016/j.yofte.2019.01.009.
- [6] Zhao, Y., Yu, C., Liao, Y. (2004). Differential FBG sensor for temperature-compensated high-pressure (or displacement) measurement, *Optics & Laser Technology*, 36(1), pp. 39-42. DOI: 10.1016/S0030-3992(03)00129-4.
- [7] Xu, M. G., Archambault, J. L., Reekie, L., Dakin, J. P. (1994). Discrimination between strain and temperature effects using dual-wavelength fibre grating sensors, *Electronics letters*, 30(13), pp. 1085-1087. DOI: 10.1049/el:19940746.
- [8] Patrick, H. J., Williams, G. M., Kersey, A. D., Pedrazzani, J. R., Vengsarkar, A. M. (1996). Hybrid fiber Bragg grating/long period fiber grating sensor for strain/temperature discrimination, *IEEE Photonics Technology Letters*, 8(9), pp. 1223-1225. DOI: 10.1109/68.531843.
- [9] Jung, J., Nam, H., Lee, J. H., Park, N., Lee, B. (1999). Simultaneous measurement of strain and temperature by use of a single-fiber Bragg grating and an erbium-doped fiber amplifier, *Applied optics*, 38(13), pp. 2749-2751. DOI: 10.1364/AO.38.002749.
- [10] Du, W. C., Tao, X. M., Tam, H. Y. (1999). Fiber Bragg grating cavity sensor for simultaneous measurement of strain and temperature, *IEEE Photonics Technology Letters*, 11(1), pp. 105-107. DOI: 10.1109/68.736409.
- [11] Guan, B. O., Tam, H. Y., Tao, X. M., Dong, X. Y. (2000). Simultaneous strain and temperature measurement using a superstructure fiber Bragg grating, *IEEE Photonics Technology Letters*, 12(6), pp. 675-677. DOI: 10.1109/68.849081.
- [12] Singh, A. K., Berggren, S., Zhu, Y., Han, M., Huang, H. (2017). Simultaneous strain and temperature measurement using a single fiber Bragg grating embedded in a composite laminate, *Smart Materials and Structures*, 26(11), pp. 115025. DOI: 10.1088/1361-665X/aa91ab.



- [13] Kipriksiz, S. E., Yücel, M. (2021). Tilted fiber Bragg grating design for a simultaneous measurement of temperature and strain, *Optical and quantum electronics*, 53(1), pp. 1-15. DOI: 10.1007/s11082-020-02609-w.
- [14] Zhang, W., Li, F., Liu, Y. (2009). FBG pressure sensor based on the double shell cylinder with temperature compensation, *Measurement*, 42(3), pp. 408-411. DOI: 10.1016/j.measurement.2008.08.007.
- [15] Morey, W. W., Meltz, G., Glenn, W. H. (1990). Fiber optic Bragg grating sensors, *Fiber optic and laser sensors VII*, 1169, pp. 98-107. DOI: 10.1117/12.963022.
- [16] Yang, T., Wang, Y., Wang, X. (2022). High-precision calibration for strain and temperature sensitivities of Rayleigh-scattering-based DOFS at cryogenic temperatures, *Cryogenics*, 124, pp. 103481. DOI: 10.1016/j.cryogenics.2022.103481
- [17] Roths, J., Andrejevic, G., Kuttler, R., Süßer, M. (2006). Calibration of fiber Bragg cryogenic temperature sensors, *Optical Fiber Sensors*, pp. TuE81. DOI: 10.1364/OFS.2006.TuE81.
- [18] Flockhart, G. M., Maier, R. R., Barton, J. S., MacPherson, W. N., Jones, J. D., Chisholm, K. E., Zhang, L., Bennion, I., Read, I., Foote, P. D. (2004). Quadratic behavior of fiber Bragg grating temperature coefficients, *Applied optics*, 43(13), pp. 2744-2751. DOI: 10.1364/AO.43.002744.
- [19] Li, G., Ji, L., Li, G., Su, J., Wu, C. (2021). High-resolution and large-dynamic-range temperature sensor using fiber Bragg grating Fabry-Pérot cavity, *Optics Express*, 29(12), pp. 18523-18529. DOI: 10.1364/OE.426398.